ACS APPLIED MATERIALS & INTERFACES

Research Article

www.acsami.org

Nanogold-Functionalized DNAzyme Concatamers with Redox-Active Intercalators for Quadruple Signal Amplification of Electrochemical Immunoassay

Jun Zhou,[†,‡] Wenqiang Lai,[†] Junyang Zhuang,[†] Juan Tang,[†] and Dianping Tang*[,†]

[†]Key Laboratory of Analysis and Detection for Food Safety (Fujian Province & Ministry of Education of China), Department of Chemistry, Fuzhou University, Fuzhou 350108, P.R. China

[‡]Modern Biochemistry Center, Guangdong Ocean University, Zhanjiang 524088, Guangdong, P.R. China

ABSTRACT: A novel and in situ amplified immunoassay strategy with quadruple signal amplification was designed for highly efficient electrochemical detection of low-abundance proteins (carcinoembryonic antigen, CEA, as a model) by using nanogold-functionalized DNAzyme concatamers with redox-active intercalators. To construct such an in situ amplification system, streptavidin-labeled gold nanoparticles (AuNP-SA) were initially used for the labelling of initiator strands (S_0) and detection antibody (mAb_2) with a large ratio (mAb_2–AuNP–S_0), and then two auxiliary DNA strands S_1 and S_2 were designed for in situ propagation of DNAzyme concatamers with the hemin/G-quadruplex format. The quadruple signal amplification was implemented by using the avidin–biotin chemistry, nanogold labels, DNA concatamers, and DNAzymes. In the presence of target CEA, the sandwiched immunocomplex was formed between the immobilized primary antibodies on the electrode and the conjugated detection antibodies on the mAb_2–AuNP–S_0. The carried S_0 initiator strands could progress a chain reaction of hybridization events between alternating S_1/S_2 DNA strands to form a nicked double-helix. Upon addition of hemin, the hemin-binding aptamers could be bound to form the hemin/G-quadruplex-based DNAzymes. The formed double-helix DNA polymers could cause the intercalation of numerous electroactive methylene blue molecules. During the electrochemical measurement, the formed DNAzymes could catalyze the reduction of H_2O_2 in the solution to amplify the electrochemical signal of the intercalated methylene blue. Under optimal conditions, the electrochemical immunoassay exhibited a wide dynamic range of 1.0 fg mL^{-1} to 20 ng mL^{-1} toward CEA standards with a low detection limit of 0.5 fg mL^{-1}. Intra-assay and inter-assay coefficients of variation (CV) were less than 8.5% and 11.5%, respectively. No significant differences at the 0.05 significance level were encountered in the analysis of 14 clinical serum specimens between the developed immunoassay and commercialized electrochemiluminescent (ECL) method for detection of CEA.

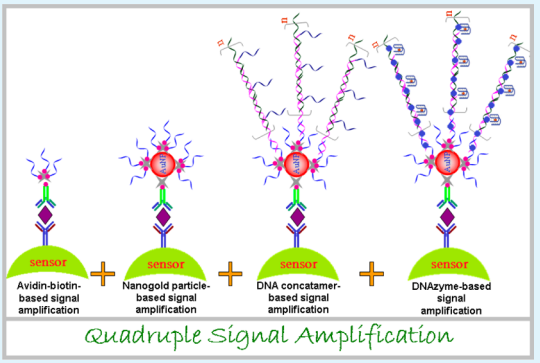

KEYWORDS: *electrochemical immunoassay, gold nanoparticles, DNAzyme concatamers, quadruple single amplification*

1. INTRODUCTION

Proteins are a general category of large molecules that serve as both structural and functional units for all living organisms. Sensitive and accurate determination of low-abundance proteins is of paramount importance in proteomics and biomedicine.[1] Typically, antibody-based immunoassay systems are versatile and powerful tools for quantifying the low-abundance proteins.[2,3] Owing to the limitation of classical analytical methodologies or instruments, however, improving the sensitivity by the traditional physical methods or simple chemical/biocatalytic process can not meet the practical demands.[4] In this regard, various signal amplification strategies have been designed and developed for improving the sensitivity of traditional immunoassays, e.g., by applying new detection probes, incorporating nanomaterials to increase the loading of tags, and making use of the enzyme-assisted amplification process.[5−10] These amplification strategies of detectable signals for highly sensitive immunoassays mainly consist of nanosignal amplification and molecular biological amplification. Notwithstanding some advances in this field, there is still the quest to explore new schemes and protocols for sensitivity improvement of clinical immunoassays, especially for some low-abundance proteins.

An alternative strategy that is based on an electrochemical principle and does not require an antibody-labeled reaction would be advantageous because of simple instrumentation and easy signal quantification.[11] Nucleic acid sequence based amplification is a primer-dependent technology that can be used for the continuous amplification of nucleic acids in a single mixture at one temperature.[12−14] A DNA concatamer, one of

Received: February 20, 2013
Accepted: March 13, 2013
Published: March 14, 2013

the linear polymeric structures that arise by self-association of short DNA fragments through specific interactions, has attracted increasing attention in molecular biology and DNA diagnostics.[15−17] Their branched 2D or 3D analogues—DNA dendrimers—have already been used to amplify the signal and enhance trapping of the query nucleic acid in hybridization analysis.[18] Recently, DNA concatamers have been for the first time reported for signal amplification of electrochemical immunoassays by our group.[19] During this process, the electrochemical signal was mainly derived from the labeled ferrocene molecules and the in situ formed DNAzymes in the concatamers toward the catalytic reaction of hydrogen peroxide in the solution. The hemin-binding aptamers exhibit electrocatalytic activity towards H_2O_2-mediated oxidation.[20−22] Despite the wide linear range and low detection limit in this method, the obtained electrochemical signal is still relatively weak (nA level in the current). The reason might most likely be as a consequence of the facts that (i) the amount of the labeled redox tags (i.e., ferrocene) in the DNAzyme concatamers is limited and (ii) the molecular tags (which could produce the electrochemical signals) are too little. To tackle these issues, our motivation of this study is to enhance the sensitivity and detectable signal of DNAzyme concatamer-based immunoassays by coupling the nanolabels with redox-active intercalators without the need of the labelling of molecular tags.

A gold nanoparticle label is an ideal candidate in the biotechnological systems due to its inherent advantages, such as easy preparation and good biocompatibility.[23,24] Methylene blue (MB), as a good redox indicator, is known to undergo binding with the nucleic acids. MB-DNA complexation has been studied both experimentally and theoretically because of methylene blue's medical importance as a photosensitizing dye.[25−27] Herein, we report the proof-of-concept of a novel and powerful electrochemical immunoassay protocol for detection of low-abundance proteins with quadruple signal amplification, e.g., carcinoembryonic antigen (CEA) [CEA is a preferred tumor marker to help predict outlook in patients with colorectal cancer, and the normal range of blood levels is lower than 3 ng mL^{-1}], by coupling nanogold-functionalized DNAzyme concatamers with redox-active intercalators as molecular tags. The assay mainly consists of the formation of sandwiched immunocomplex, the DNA concatamer hybridization reaction, the formation of hemin-binding G-quadruplex DNAzymes, the indicator intercalation, and electrochemical measurement.

2. EXPERIMENTAL SECTION

CEA was purchased from Biocell Biotechnol. Co., Ltd. (Zhengzhou, China). Monoclonal mouse anti-human CEA antibody (clone II-7, designated as mAb_1, dilution: 1:25−1:50) was obtained from Dako Diagnostics Co., Ltd. (Shanghai, China). Biotinylated monoclonal mouse anti-human CEA antibody (clone M0911042, 9.0 mg mL^{-1}) (designated as bio-mAb_2) was achieved from MyBioSource Inc. (San Diego, USA). Streptavidin (SA) was purchased from Amyjet Scientific, Inc. (Wuhan, China). β-Cyclodextrin (CD) was obtained from Sinopharm Chem. Re. Co. (Shanghai, China). The biotinylated initiator strand (bio-S_0), S_1, and S_2 were obtained from Sangon Biotech. Co., Ltd. (Shanghai, China). The sequences of oligonucleotides are listed as follows:

Bio-S_0: 5′-biotin-$(CH_2)_6$-GTACT ACAGC AGCTG-3′

S_1: 5′-GGG TAGGG CGGGT TGGGT *ATCTC CTAAT AGCAG* CAGCT GCTGT AGTAC-3′

S_2: 5′-*CTGCT ATTAG GAGAT* GTACT ACAGC AGCTG-3′

In the probe S_1, the hemin-binding aptamer is the 18-nt bases at the 5′ end. The underlined sequence of probe S_2 at the 3′ end is the same as probe S_0, which is complementary to the underlined sequence of probe S_1 at the 3′ end. The italic letters of probe S_1 in the middle are the sequence complementary to the italic letters of probe S_2 at the 5′ end. DNA stock solution was obtained by dissolving oligonucleotides in tris-HCl buffer solutions (pH 7.4). Each oligonucleotide was heated to 90 °C for 5 min and slowly cooled to room temperature before usage. Gold colloids with 16 nm in diameter were prepared and characterized as described.[28] All other reagents were of analytical grade and were used without further purification. Ultrapure water obtained from a Millipore water purification system (≥18 MΩ, Milli-Q, Millipore) was used in all runs. Clinical serum samples were made available by Fujian Provincial Hospital, China. Phosphate-buffered saline (PBS, 0.1 M) solution with various pHs was prepared by mixing the stock solutions of 0.1 M NaH_2PO_4 and 0.1 M Na_2HPO_4, and 0.1 M KCl was added as the supporting electrolyte.

Prior to bioconjugation, streptavidin-labeled gold nanoparticles (AuNP-SAs) were prepared according to the literature with a little modification.[29] Briefly, 5 mL of gold colloids (AuNP, $C_{[Au]}$ = 24 μM) was adjusted to pH 7.6 by directly using 0.1 M Na_2CO_3 aqueous solution. Then, 0.5 mL of streptavidin aqueous solution (10 mg mL^{-1}) was added into the resulting gold colloids. After gentle shaking on the shaker (MS, IKA GmbH, Staufen, Germany) for 1 h at room temperature (RT), 110 μL of 1.0 wt % polyethylene glycol was injected, and the mixture was further incubated overnight. During this process, the association of streptavidin onto the surface of nanogold particles is possibly due to the interaction between cysteine or NH_3^+-lysine residues of streptavidin and gold nanoparticles.[30] Following that, the resultant mixture was repeatedly centrifuged at 4 °C for 20 min (14 000*g*). The obtained precipitate (AuNP-SA) was redispersed in 1.0 mL of PBS (0.1 M, pH 7.4).

Next, the as-synthesized AuNP-SA was used for preparation of mAb_2−AuNP−S_0 detection antibodies by consulting the literature.[2] Initially, 50 μL of bio-mAb_2 (1.0 μM) was added into the as-prepared AuNP-SA suspension and incubated for 20 min at RT. Afterwards, 200 μL of bio-S_0 (100 μM) was injected into the mixture. After gently shaking for 5 min, the mixture was transferred to the refrigerator at 4 °C for further reaction (overnight). During this process, bio-mAb_2 and bio-S_0 were covalently bound to AuNP-SA via the classical avidin−biotin reaction.[31,32] Following that, the mixture was centrifuged (14 000*g*) for 10 min at RT. The pellet (i.e., mAb_2−AuNP−S_0) was resuspended in 1.0 mL of 2 mM sodium carbonate solution containing 1.0 wt % BSA and 0.1% sodium azide, pH 7.4, and stored at 4 °C until use.

A glassy carbon electrode (GCE) with 2 mm in diameter was polished with 0.3 μm and 0.05 μm alumina, followed by successive sonication in bidistilled water and ethanol for 5 min, and dried in air. The well-polished electrode was cycled in a 0.1 M H_2SO_4 solution 5 times in the potential range from 0 to 2 V. During this process, the anodization of the GCE surface resulted in a multilayer oxide film having −OH groups or −COOH groups.[33] Following that, 5 μL of β-cyclodextrin

Scheme 1. Schematic Representation of Nanogold-Functionalized DNAzyme Concatamers with Redox-Active Intercalators for Quadruple Signal Amplification of Electrochemical Immunoassays: Adivin−Biotin Chemistry with First Signal Amplification, AuNP-Based Second Signal Amplification, DNA Concatamer-Based Third Signal Amplification, and DNAzyme-Based Fourth Signal Amplification

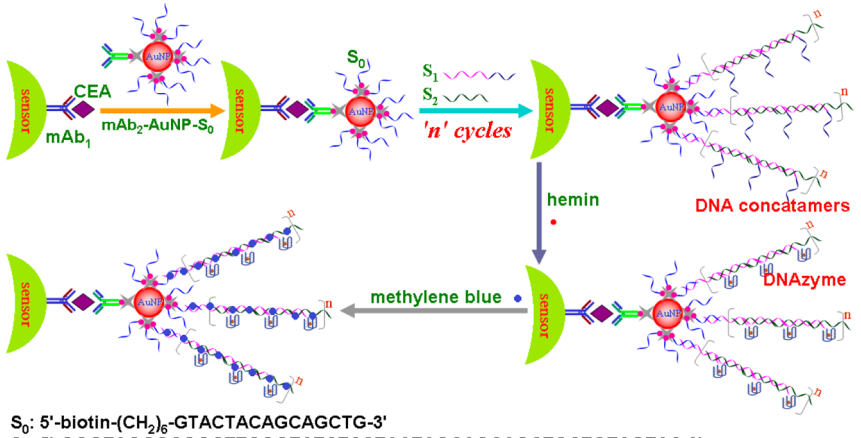

(CD) aqueous solution (50 mg mL^{-1}) was cast onto the surface of the pretreated GCE and dried for about 2 h at RT to form a CD-modified GCE. After washing with distilled water, 30 μL of mAb_1 antibodies (dilution ratio: 1:50) was thrown on the modified electrode and incubated for 4 h at RT. During this process, mAb_1 antibodies were immobilized on the CD-modified GCE owing to the β-cyclodextrin capture.[34,35] Finally, the as-prepared mAb_1−CD−GCE was stored at 4 °C when not in use.

Scheme 1 gives the schematic illustration of the electrochemical immunoassay protocols based on nanogold-functionalized DNAzyme concatamers. In this work, all electrochemical measurements were carried out on an AutoLab electrochemical workstation (μAUTIII.FRA2.v, Eco Chemie, The Netherlands). A conventional three-electrode system used in the measurements consists of a modified GCE working electrode, a platinum foil auxiliary electrode, and a saturated calomel electrode (SCE) as reference electrode. The assay was performed as follows: (i) *immunoreaction*: 10 μL of incubation solution including various-concentration CEA samples and mAb_2−AuNP−S_0 ($C_{[Au]}$ = 120 μM) was dropped onto the surface of mAb_1−CD−GCE and incubated for 40 min at RT to form a sandwiched immunocomplex; (ii) *hybridization reaction*: the resulting immunosensor was immersed (*Note*: suspended) into the hybridization solution containing 0.5 μM S_1 and 0.5 μM S_2 and incubated for 80 min at RT (*Note*: During this process, the hybridization reaction was triggered and progressed to form the long nicked DNA concatamers on the AuNP); (iii) *DNAzyme formation*: the modified electrode was suspended into 0.2 mM hemin solution and reacted for 50 min at RT to form the hemin/G-quadruplex (i.e., DNAzyme) complex; (iv) *intercalation of methylene blue*: the resultant immunosensor was suspended into the 0.5 mM methylene blue aqueous solution and incubated for 30 min at RT (*Note*: During this process, the methylene blue molecules were intercalated into the grooves of the double-helix); and (v) *electrochemical measurement*: the electrochemical characteristics of the resulting immunosensors were investigated by differential pulse voltammetry (DPV) from 0 to −500 mV (vs SCE) in the PBS (pH 7.0) containing 3.0 mM H_2O_2. After each step, the immunosensor was washed by using pH 7.4 PBS. Analyses are always made in triplicate.

3. RESULTS AND DISCUSSION

In this work, the immunosensor was simply prepared by means of immobilizing mAb_1 on the β-cyclodextrin-modified GCE based on the host−guest chemistry, while the streptavidin-labeled AuNPs were heavily functionalized with bio-S_0 and bio-mAb_2, which were utilized as the detection antibodies (mAb_2-AuNP−S_0). Two auxiliary DNA strands (S_1 and S_2) were designed for the concatamer reaction. In the design, the 30 bases at the 3′ end of S_1 are completely complementary with S_2. Differently, the beginning 18 nt at the 5′ end of S_1 can bind with hemin to form the DNAzyme. It is noted that the 15 bases at the 3′ end of S_2 are also complementary with the primer S_0 on the AuNPs. In a typical target CEA detection experiment, the mAb_1−CD−GCE and mAb_2−AuNP−S_0 initially sandwich the target CEA, generating a complex with a large ratio of S_0 and target CEA. The carried initiator stands on the mAb_2−AuNP−S_0 can propagate a chain reaction of hybridization events between alternating S_1 and S_2 in sequence to form a nicked double-helix. Upon addition of hemin, the hemin-binding aptamers can be bound to form the hemin/G-quadruplex-based DNAzymes. Hence, a large number of DNAzymes are concatamerized via the double-helix DNA. Meanwhile, the formed double-helix DNA polymers cause the intercalation of numerously electroactive methylene blue into the grooves. In this case, the intercalated methylene blue molecules are brought into close proximity with each other on the concatamers, thereby resulting in the formation of numerous methylene blue molecules and DNAzymes. During the measurement, the formed DNAzymes can catalyze the reduction of H_2O_2 with the aid of methylene blue. The catalytic currents directly depend on the concentration of target CEA in the sample. In the absence of target CEA, mAb_2−AuNP−S_0 can not be conjugated onto the mAb_1−CD−GCE, thus displaying a relatively low background signal.

As mentioned above, the electrochemical signal was mainly derived from the intercalated methylene blue and the formed DNAzymes on the mAb_2−AuNP−S_0. To realize our design, we first used transmission electron microscopy (TEM, H-7650,

Hitachi Instruments, Japan) and gel electrophoresis (Sub-Cell GT Agarose Gel Electrophoresis systems, Bio-Rad Laboratories, Inc., USA) to characterize the mAb_2–AuNP–S_0 before and after incubation with S_1 + S_2 (*Note*: the TEM image after hybridization was obtained by dyeing). As shown from Figure 1a, the long nicked DNA polystrands could be observed on the

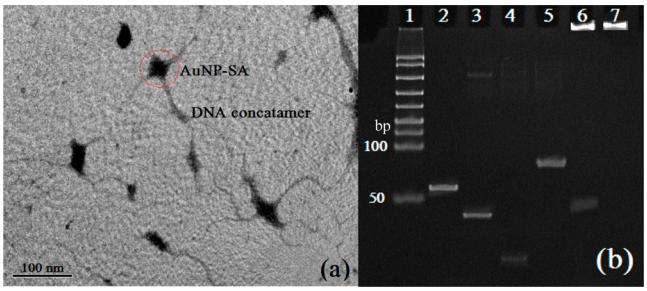

Figure 1. (a) TEM image of mAb_2–AuNP–S_0 after incubation with S_1 and S_2 probes and (b) gel electrophoresis (lane 1: DNA ladder; lane 2: 0.1 μM S_1; lane 3: 0.1 μM S_2; lane 4: 0.1 μM S_0; lane 5: 0.1 μM S_1 + 0.1 μM S_2; lane 6: 0.1 μM S_2 + mAb_2–AuNP–S_0; lane 7: 0.1 μM S_1 + 0.1 μM S_2 + mAb_2–AuNP–S_0).

AuNPs after hybridization with S_1 + S_2. The results indicated that DNA concatamers could be formed in the presence of S_1 + S_2 with the guidance of the initiator strands on the mAb_2–AuNP–S_0. Figure 1b shows typical gel electrophoresis of various components. As seen from lanes 2–4, the base numbers of S_1, S_2, and S_0 oligonucleotides were very close to our design. Significantly, it can be seen that one ~80-nt spot was acquired at the incubation solution containing 0.1 μM S_1 and 0.1 μM S_2 (lane 5), which was attributed to the formation of DNA concatamers due to their self-hybridization reaction. As a control test, the incubation solution containing 0.1 μM S_2 and mAb_2–AuNP–S_0 was implemented. As shown from lane 6, two spots were achieved for S_1 and mAb_2–AuNP–S_0, respectively, suggesting that the mixture containing S_1 and mAb_2–AuNP–S_0 could not cause their self-hybridization. The reason for a strong spot at the beginning of lane 6 might be the fact that the as-prepared mAb_2–AuNP–S_0 was difficultly migrated during the gel electrophoresis. When 0.1 μM S_1, 0.1 μM S_2, and excess mAb_2–AuNP–S_0 were simultaneously present in the incubation solution, inspiringly, one strong spot at the beginning of lane 7 was obtained. The reason might be most likely as a consequence of the fact that the added S_1 and S_2 were consumed as a result of a chain reaction of hybridization events to form DNA concatamers on the mAb_2–AuNP–S_0. These results revealed that the DNA concatamers could be progressed in the simultaneous presence of S_1/S_2/mAb_2–AuNP–S_0, thus providing a precondition for the formation of DNAzyme concatamers on the mAb_2–AuNP–S_0.

Logically, another question arises as to whether the formed DNA concatamers on the mAb_2–AuNP–S_0 could induce the construction of DNAzyme concatamers and the intercalation of methylene blue on the DNA concatamers. To investigate these issues, the as-prepared mAb_1–CD–GCE was used for the detection of 1.0 ng mL^{-1} of CEA by using nanogold-labeled DNAzyme concatamers as molecular tags with a sandwich-type immunoassay format. Figure 2A shows cyclic voltammograms of variously modified mAb_1–CD–GCE in pH 7.0 PBS at 50 mV s^{-1}. No redox peaks were observed after the newly prepared mAb_1–CD–GCE was incubated with 1.0 ng mL^{-1} of CEA, mAb_2–AuNP–S_0, and S_1 + S_2 in sequence (curve '*a*'). The results indicated that the immobilized biomolecules and AuNPs did not have redox properties. When the resulting immunosensor was reincubated with hemin, however, a pair of very weak redox peaks was observed (curve '*b*'), which mainly derived from the direct electron transfer of the immobilized hemin.[36] Especially, when methylene blue molecules with good redox activity were intercalated into the DNAzyme concatamers, a couple of stable and well-define redoxes at −240 and −330 mV were acquired (curve '*c*'). Favorably, upon addition of 3.0 mM H_2O_2 in pH 7.0 PBS, an obvious catalytic characteristic appeared with a dramatic increase of reduction current and a sharp decrease of oxidation current (curve '*d*'). The result indicated that the formed DNAzymes in the concatamers could exhibit an obvious enzymatic catalytic behavior. The increase of the reduction current was mainly derived from the DNAzymes toward the catalytic reduction of H_2O_2 with the help of methylene blue electron mediators. Hence, the DNAzyme concatamers could be used for the signal amplification of the electrochemical immunoassays.

To further investigate that the intercalated methylene blue in the DNAzyme concatamers could exhibit good conductivity, Faradic electrochemical impedance spectroscopy (EIS) was employed to investigate the interface properties of the modified electrode before and after the intercalation of methylene blue in the DNAzyme concatamer-modified immunosensor in 5.0 mM

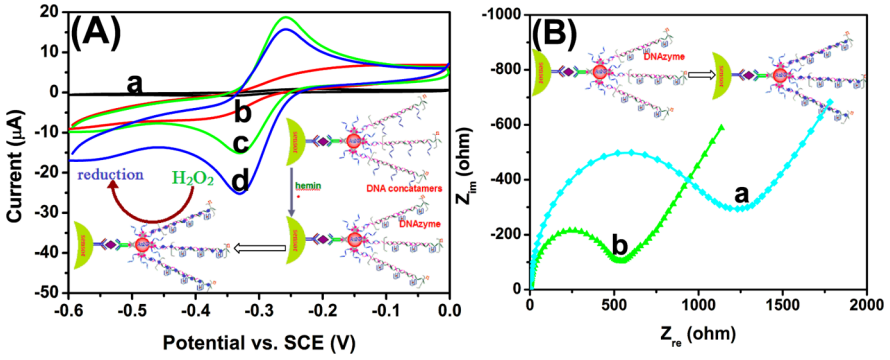

Figure 2. (A) Cyclic voltammograms of variously modified electrodes: (a) mAb_1–CD–GCE after incubation with 1.0 ng mL^{-1} of CEA/mAb_2–AuNP–S_0/(S_1 + S_2) in pH 7.0 PBS, (b) electrode '*a*' after reaction with hemin in pH 7.0 PBS, (c) electrode '*b*' after intercalation of methylene blue in pH 7.0 PBS, and (d) electrode '*c*' in pH 7.0 PBS containing 3.0 mM H_2O_2. (B) Nyquist diagrams for (a) mAb_1–CD–GCE after incubation with 1.0 ng mL^{-1} of CEA/mAb_2–AuNP–S_0/(S_1 + S_2)/hemin and (b) electrode '*a*' after intercalation of methylene blue in 5.0 mM $Fe(CN)_6^{4-/3-}$ + 0.1 M KCl with the range from 10^{-2} to 10^5 Hz at an alternate voltage of 5 mV.

dx.doi.org/10.1021/am400652g | *ACS Appl. Mater. Interfaces* 2013, 5, 2773–2781

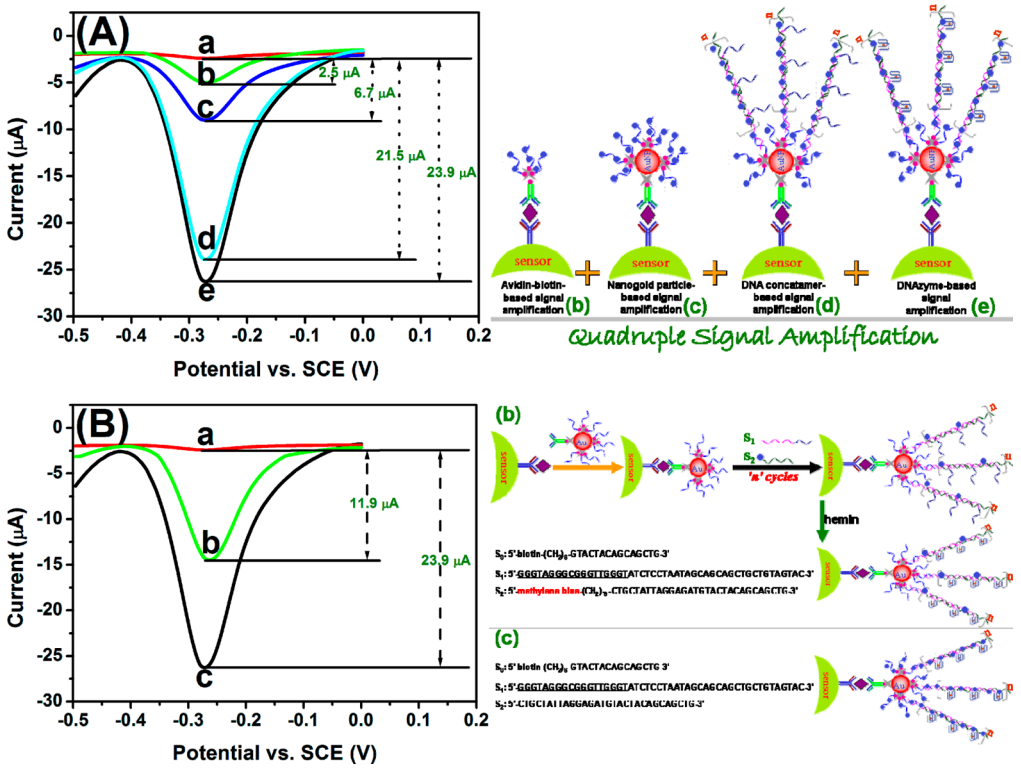

Figure 3. (A) DPV response curves of the as-prepared mAb_2−CD−GCE toward 1.0 ng mL^{-1} of CEA by using various molecular tags: (a) mAb_2-bio, (b) mAb_2-bio/SA/bio-S_0, (c) mAb_2-bio/AuNP-SA/bio-S_0, (d) mAb_2-bio/AuNP-SA/bio-S_0/$\{S_1 + S_2\}_n$, and (e) mAb_2-bio/AuNP-SA/bio-S_0/$\{S_1 + S_2 + \text{hemin}\}_n$ in pH 7.0 PBS containing 3.0 mM H_2O_2 (n = 3). (B) Comparison of DPV responses of the as-prepared mAb_2−CD−GCE toward 1.0 ng mL^{-1} of CEA by using various immunoassay modes: (a) methylene blue-labelling strategy and (b) methylene blue-intercalated strategy in pH 7.0 PBS containing 3.0 mM H_2O_2 (n = 3).

$Fe(CN)_6^{4-/3-}$ containing 0.1 M KCl (Figure 2B). Curve '*a*' in Figure 2B represents the Nyquist diagram of the mAb_1−CD−GCE after incubation with 1.0 ng mL^{-1} of CEA, mAb_2−AuNP−S_0, S_1 + S_2, and hemin in turn. The resistance, R_{et}, was 1263 Ω. When the modified electrode was incubated with methylene blue, however, the resistance was decreased (R_{et} = 521 Ω) (curve '*b*'). The reason was that the intercalated methylene blue molecules could serve as an intervening "spacer" matrix to extend the immobilized biomolecules away from the substrate matrix in the mobile phase, resulting in binding sites more accessible to biomolecules.

To investigate the nanogold-labeled DNAzyme concatamers with redox-active intercalators for quadruple signal amplification of the developed electrochemical immunoassay, four types of molecular tags, including mAb_2-bio/SA/bio-S_0, mAb_2-bio/AuNP-SA/bio-S_0, mAb_2-bio/AuNP-SA/bio-S_0/$\{S_1 + S_2\}_n$, and mAb_2-bio/AuNP-SA/bio-S_0/$\{S_1 + S_2 + \text{hemin}\}_n$, were used for detection of 1.0 ng mL^{-1} of CEA (as an example) on the same-batch mAb_1−CD−GCE under the same experimental conditions (Figure 3A). The evaluation was made by comparison with the change in the peak currents relative to zero analyte in pH 7.0 PBS containing 3.0 mM H_2O_2. As a control test, mAb_2-bio tags were initially used for detection of 1.0 ng mL^{-1} of CEA, followed by the intercalation of methylene blue, to monitor whether methylene blue molecules could be nonspecifically adsorbed onto the bio-pAb_2/CEA/mAb_1−CD−GCE. Experimental results indicated that almost no obvious peaks were changed before and after incubation with methylene blue (curve '*a*'), thus the nonspecific absorption was negligible. When using mAb_2-bio/SA/bio-S_0 as molecular tags, the shift in the currents was 2.5 μA (curve '*b*' vs curve '*a*'). The reason was ascribed to the four binding sites of streptavidin (one for mAb_2-bio vs three for bio-S_0). The carried S_0 initiator strands with negative charge could adsorb the positively charged methylene blue, resulting in the appearance of electrochemical signal. Significantly, the electrochemical signal could be further improved when using mAb_2-bio/AuNP-SA/bio-S_0 as molecular tags (curve '*c*' vs curve '*a*'). The reason might be the fact that gold nanoparticles have a large surface coverage and hence exhibit a high conjugation capacity for bio-S_0. Herein, we might roughly estimate that one streptavidin tetramer could simultaneously conjugate three bio-S_0 molecules at most, while one 16 nm AuNP could simultaneously accommodate up to 64 streptavidin tetramers (*Note*: The calculation is based on the spherical surface area $[S_{NP} = 4\pi r_{NP}^2]$ divided by the area of the streptavidin's radius-based circle $[S_{streptavidin} = \pi r_B^2]$, where r_{NP} stands for the radius of AuNPs and r_B stands for the radius of the streptavidin [4−5 nm in diameter][37,38]). Therefore, more bio-S_0 molecules (64 × 3 = 192, according to one site for AuNP and three for bio-S_0) could be simultaneously conjugated onto the AuNP-SA nanoparticles than a single streptavidin tetramer. When one mAb_2 antibody on the mAb_2−AuNP−S_0 reacted with the corresponding antigen, the whole initiator strand on the mAb_2−AuNP−S_0 would be carried over and thus participate in the interaction with methylene blue, thus displaying high electrochemical signal. Further, the electrochemical signals could be greatly amplified when using mAb_2-bio/AuNP-SA/bio-S_0/$\{S_1 + S_2\}_n$ (curve '*d*') and mAb_2-bio/AuNP-SA/bio-S_0/$\{S_1 + S_2 + \text{hemin}\}_n$ (curve '*e*') as molecular tags, respectively. The reason might be

dx.doi.org/10.1021/am400652g | ACS Appl. Mater. Interfaces 2013, 5, 2773−2781

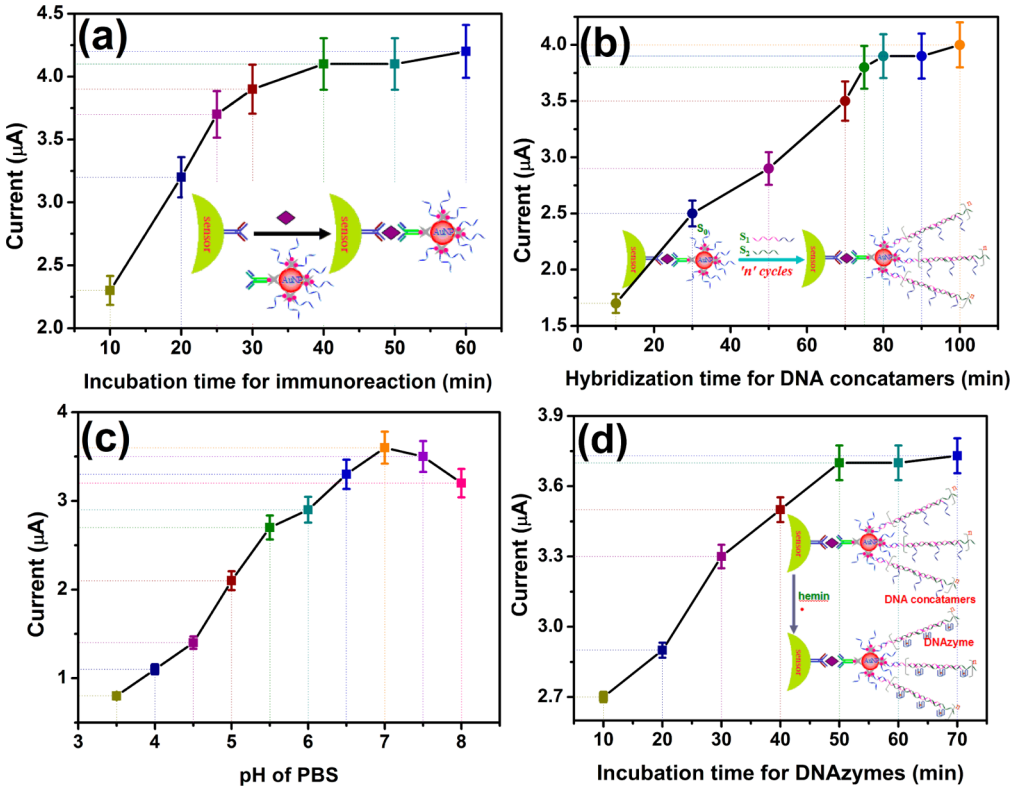

Figure 4. (a) Signal dependence of the developed electrochemical immunoassays on (a) incubation time for antigen−antibody reaction, (b) hybridization time of DNA concatamers, (c) pH of PBS, and (d) incubation time for DNAzymes by using 10 fg mL^{-1} of CEA as an example.

the facts that (i) methylene blue molecules could be intercalated into between adjacent base pairs or into the minor or the major groove of the DNA helix and (ii) the formed hemin/G-quadruplex DNAzymes could act as peroxidase-mimicking enzymes, which could catalyze the reduction of H_2O_2 with the aid of methylene blue mediators.

Maybe, a universal question to be produced was why not to use the labelling of methylene blue on the S_1 or S_2 but to utilize their intercalation approach into the DNA concatamers. To elucidate this issue, the methylene blue-labeled S_2 at the end of 5′ (i.e., similar to our recently reported mode[19]) was also used for detection of 1.0 ng mL^{-1} of CEA. The judgement was based on the change in the DPV peak currents relative to zero analyte. As seen from Figure 3B, the immunoassay using the methylene blue labelling strategy exhibited a relatively weak current response (Δi = 11.9 μA, curve '*b*' vs curve '*a*'). In contrast, a high peak current was achieved by using the methylene blue intercalating strategy (Δi = 23.9 μA, curve '*c*' vs curve '*a*'). Therefore, the methylene blue intercalating method could cause a 200.8 ± 4.3% signal increase of the developed immunoassay relative to the methylene blue labelling probes. This is most likely a consequence of the fact that the intercalated amount of methylene blue in the DNA concatamers was much more than that of the labeled methylene blue. We might also roughly estimate that a double-stranded DNA with 30 base pairs (30 nucleotides for DNA concatamers between S_1 and S_2 in this work) could label only one methylene blue due to the presence of one 5′ end of S_2. In contrast, such a double-helix structure could form three major grooves and three minor grooves at least (*Note*: The double helix is right-handed with about 10−10.5 nucleotides per turn),[39] which could accommodate six methylene blue molecules. More importantly, every initiator strand on the AuNPs could trigger the formation of a long nicked DNA polymer, thereby resulting in the intercalation of numerous methylene blue molecules, thus enhancing the electrochemical response signal.

On the basis of the results in Figure 3, we might clearly observe that the quadruple signal amplification of the electrochemical immunoassays could be implemented by using streptavidin tetramers (1st amplification), AuNPs (2nd amplification), DNA concatamers (3rd amplification), and DNAzymes (4th amplification).

To achieve the optimal analytical properties of the electrochemical immunoassays, some experimental parameters including incubation time and incubation temperature for the antigen−antibody reaction, the hybridization time of DNA concatamers, the binding time between hemin/G-quadruplex, and pH of the assay solution should be studied. In these cases, 10 fg mL^{-1} of CEA was used as an example. Usually, the antigen−antibody reaction is adequately carried out at human normal body temperature (37 °C). Considering the possible application of the developed immunoassay in the future, we selected room temperature (25 ± 1.0 °C) for the antigen−antibody interaction throughout the experiment. At this condition, we monitored the effect of incubation time on the currents of the immunosensors from 10 to 60 min (*Note*: To avoid confusion, the incubation times of the immunosensor with CEA were paralleled with those of the immunosensor−CEA with mAb_2−AuNP−S_0). As shown in Figure 4a, the DPV peak currents increased with the increment of incubation time and tended to level off after 40 min. Hence, an incubation time of 40 min was selected for determination of CEA at acceptable throughput.

Figure 4b displays the effect of hybridization time between mAb_2–AuNP–S_0 and S_1 + S_2 on the electrochemical signal of the immunoassay. The current increased with the time aged and tended to level off after 80 min. Meanwhile, we also monitored the effect of binding time between hemin/G-quadruplex on the signal of the electrochemical immunoassays. An acceptable signal was obtained at ~50 min, as shown in Figure 4c. Longer incubation time did not cause the large change in the current. Therefore, 80 min and 50 min were used for the construction of DNA concatamers and the formation of DNAzymes on the mAb_2–AuNP–S_0.

To maintain the bioactivity of the DNAzymes and adequately fulfill its catalytic potential, a moderately acidic pH should be preferable. Figure 4d displays the dependence of DPV peak currents on pH of PBS. An optimal current was obtained at pH 7.0 PBS. Higher or lower pHs resulted in the decrease of cathodic currents. Thus, a pH 7.0 PBS was chosen as the supporting electrolyte.

Under the optimal conditions, the sensitivity and working range of the electrochemical immunoassay were studied by assaying routine samples with different CEA standards by using mAb_2-bio/AuNP-SA/bio-S_0/$\{S_1 + S_2 + \text{hemin}\}_n$ as molecular tags. The DPV peak currents increased with the increasing CEA level in the sample solution (Figure 5). A linear dependence

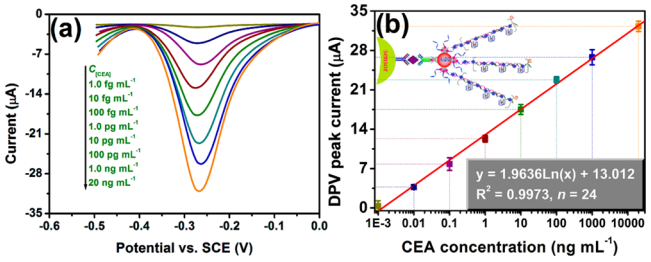

Figure 5. (a) Typical DPV response curves of the electrochemical immunoassays for different target CEA standards by using nanogold-functionalized DNAzyme concatamers as molecular tags and (b) the corresponding linear curves.

between the peak currents and the logarithm of CEA levels was obtained in the range from 1.0 fg mL^{-1} to 20 ng mL^{-1}, i.e., over seven decades. The linear regression equation was Δi (μA) = 1.9636 × log $C_{[CEA]}$ + 13.012 (pg mL^{-1}) (R^2 = 0.9973, n = 24) with a detection limit (LOD) of 0.5 fg mL^{-1} at the $3s_{blank}$ criterion. For comparison, we also investigated the analytical properties of the electrochemical immunoassays by using mAb_2-bio/streptavidin/bio-S_0/$\{S_1 + S_2 + \text{hemin}\}_n$ and mAb_2-bio/AuNP-SA/bio-S_0/$\{S_1 + S_2\}_n$, respectively. The linear range and LOD were 0.5–20 ng mL^{-1} and 0.1 ng mL^{-1} and 0.01–20 ng mL^{-1} and 5.0 pg mL^{-1}, respectively. Although the system has not yet been optimized for maximum efficiency, the LOD using mAb_2-bio/AuNP-SA/bio-S_0/$\{S_1 + S_2 + \text{hemin}\}_n$ was four to six orders of magnitude lower than those without AuNP or hemin. The results further demonstrated the amplified efficiency of the nanogold-functionalized DNAzyme concatamers toward the developed electrochemical immunoassay system.

The precision and reproducibility of the electrochemical immunoassays were investigated by repeatedly assaying three different CEA concentrations, using identical batches of mAb_1–CD–GCE and mAb_2–AuNP–S_0. Experimental results revealed that the coefficients of variation (CVs) of the intra-assay between five runs were 7.2%, 5.3%, and 8.2% for 5.0 fg mL^{-1}, 5.0 pg mL^{-1}, and 5.0 ng mL^{-1} CEA, respectively; the batch-to-batch reproducibility with various batches was studied, and the CVs were 11.3%, 8.4%, and 9.5% towards the above-mentioned levels, respectively. With the exception of the slightly increased CV for the 5.0 fg mL^{-1} standard in the inter-assay experiment, the other CVs indicated that the electrochemical immunoassay could be used repeatedly and further verified the possibility of batch preparation. When the mAb_1–CD–GCE and mAb_2–AuNP–S_0 were stored at 4 °C and measured intermittently (every 3–5 days), they could maintain 96.4%, 89.7%, and 81.3% of the initial signal after being stored for 10, 20, and 30 days, respectively. We speculate that the slow decrease of the signals was mainly attributed to the gradual deactivation of the immobilized biomolecules.

To investigate the interfering effects of sample matrix components on the responses of our developed strategy, we challenged the system with several possible components in the normal human serum samples since these samples usually co-exist in the normal human serum, such as K^+, Ca^{2+}, Cl^-, HCO_3^-, glucose (Glu), uric acid (UA), dopamine (DA), and α-fetoprotein (AFP). The comparative study was carried out by measuring the low concentration of target CEA and high concentration of interfering components based on the change in the current before and after addition of the interfering reagents. As indicated from Figure 6, higher current was observed with the target CEA than those of other components. These results clearly demonstrated the high specificity of the electrochemical immunoassays.

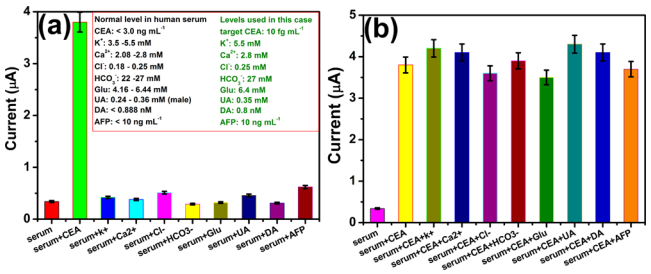

Figure 6. Interfering effects of sample matrix components on the electrochemical signal of the developed immunoassays. Initially, normal human serum samples used for spiking were assayed by using the electrochemical immunoassay, and various sample matrices were then spiked into the serum samples. Following that, the resulting mixtures were determined by using the same method. *Note*: Using the spiking level for each interfering component was near the maximum concentration of the normal human serum in this case.

To investigate the analytical reliability and potential applicability of the electrochemical immunoassay for testing real samples, we collected 14 human serum specimens with various CEA concentrations from Fujian Provincial Hospital of China according to the rules of the local ethical committee. Prior to measurement, these samples were gently shaken at room temperature (*Note*: all handing and processing was performed carefully, and all tools in contact were disinfected after use) and then monitored by using the developed electrochemical immunoassay. The results were compared with those obtained by using the commercialized electrochemiluminescence immunoassay (ECLIA) method. The obtained levels of CEA in these samples by the developed immunoassays displayed the deviations ranging from 3.1% to 9.8% (Table 1). The statistical analysis of these experimental

dx.doi.org/10.1021/am400652g | ACS Appl. Mater. Interfaces 2013, 5, 2773–2781

Table 1. Comparison of the Obtained Results for Human Serum Specimens by Using the Developed Electrochemical Immunoassay and the Reference ECLIA Method[a]

	electrochemical immunoassay	ECLIA	
sample no.[b]	$C_{[CEA]}$ (mean ± SD, ng mL^{-1})[c]	$C_{[CEA]}$ (mean ± SD, ng mL^{-1})	t_{exp}
1	14.5 ± 1.38	15.3 ± 1.3	0.73
2	56.7 ± 2.55	53.2 ± 3.03	1.53
3	93.2 ± 6.8	98.4 ± 6.4	0.96
4	5.3 ± 0.28	4.8 ± 0.3	2.12
5	23.4 ± 1.94	26.3 ± 1.29	2.15
6	47.6 ± 3.43	43.4 ± 2.95	1.61
7	32.1 ± 3.02	30.2 ± 2.45	0.85
8	19.3 ± 0.81	20.6 ± 1.5	1.32
9	6.8 ± 0.21	7.5 ± 0.39	2.73
10	29.5 ± 2.42	31.7 ± 2.19	1.17
11	37.8 ± 3.7	36.2 ± 2.46	0.62
12	126.2 ± 4.29	121.9 ± 10.12	0.68
13	87.4 ± 4.54	86.8 ± 6.42	0.13
14	11.2 ± 0.87	12.3 ± 0.76	1.64

[a]The regression equation (linear) for these data is as follows: $y = 0.9806x + 0.6316$ ($R^2 = 0.9945$, $n = 42$; x axis: by the electrochemical immunoassay; y axis: by ECLIA). [b]Analyses were made in triplicate, and the data were obtained as mean values of three assays ($n = 3$). [c]The concentrations (>20 ng mL^{-1}) were calculated by multiplying the dilution factor.

results was performed by using a t-test and a linear regression analysis approach between two methods at the 0.05 significance level. As indicated from Table 1, the t_{exp} values in all cases were less than t_{crit} ($t_{crit[4, 0.05]} = 2.77$),[40] while the slope and intercept of the regression equation between the two methods were close to the ideal unities of '0' and '1'.

To further highlight the merits of the developed electrochemical immunoassay for detection of CEA samples with the ultra-low concentrations, 4.8 ng mL^{-1} of the CEA clinical serum sample mentioned above (obtained by ECLIA, as an example) was diluted to 4.8 fg mL^{-1}, 48 fg mL^{-1}, 480 fg mL^{-1}, 4.8 pg mL^{-1}, and 48 pg mL^{-1} by using newborn calf serum, respectively. The levels measured by the electrochemical immunoassays were 5.2 fg mL^{-1}, 46.7 fg mL^{-1}, 512.3 fg mL^{-1}, 5.3 pg mL^{-1}, and 45.2 pg mL^{-1} for the above-mentioned concentrations, respectively. The recoveries were 108.3, 97.3, 106.7, 110.4, and 94.2%, respectively. These results revealed that the amplified electrochemical immunoassay could provide assay performance comparable to the commonly used method and could be considered as an optional scheme for detection of CEA in clinical diagnostics.

4. CONCLUSIONS

In summary, we have developed an in situ amplified immunoassay method for highly sensitive electrochemical detection of low-abundance proteins in biological fluids by coupling with the amplifying functionality of DNAzyme concatamers and the classical avidin−biotin amplification system with the nanogold-based labelling technique. The in situ formed DNAzyme concatamers on the nanogold particles could further amplify the detectable signal with the help of the intercalated methylene blue molecules. More favorably, the DNA-based hybridization chain reaction, an excellent isothermal signal-amplification technique, does not require the participation of an enzyme. In addition, the methodology does not involve the sophisticated fabrication and is well suited for highly sensitive biomedical sensing and application in both clinical diagnostics by controlling the target antibody.

AUTHOR INFORMATION

Corresponding Author

*Phone: +86-591-22866125. Fax: +86-591-22866135. E-mail: dianping.tang@fzu.edu.cn.

Notes

The authors declare no competing financial interest.

ACKNOWLEDGMENTS

Support by the "973" National Basic Research Program of China (2010CB732403), the Research Fund for the National Science Foundation of Fujian Province (2011J06003), the Doctoral Program of Higher Education of China (20103514120003), the National Natural Science Foundation of China (21075019 and 41176079), and the Program for Changjiang Scholars and Innovative Research Team in University (IRT1116) is gratefully acknowledged.

REFERENCES

(1) Fonslow, B.; Stein, B.; Webb, K.; Xu, T.; Choi, J.; Park, S.; Yates, J. *Nat. Methods* **2013**, *10*, 54−56.
(2) Zhang, B.; Liu, B.; Tang, D.; Niessner, R.; Chen, G.; Knopp, D. *Anal. Chem.* **2012**, *84*, 5392−5399.
(3) Feng, L.; Bian, Z.; Peng, J.; Jiang, F.; Yang, G.; Zhu, Y.; Yang, D.; Jiang, L.; Zhu, J. *Anal. Chem.* **2012**, *84*, 7810−7815.
(4) Ju, H. *J. Biochips Tissue Chips* **2012**, *2*, e114.
(5) Liang, G.; Liu, S.; Zou, G.; Zhang, X. *Anal. Chem.* **2012**, *84*, 10645−10649.
(6) Yuan, L.; Xu, L.; Liu, S. *Anal. Chem.* **2012**, *84*, 10737−10744.
(7) Li, Y.; Ma, M.; Zhu, J. *Anal. Chem.* **2012**, *84*, 10492−10499.
(8) Martic, S.; Gabriel, M.; Turowec, J.; Litchfield, D.; Kraatz, H. *J. Am. Chem. Soc.* **2012**, *134*, 17036−17045.
(9) Zhou, J.; Xu, M.; Tang, D.; Gao, Z.; Tang, J.; Chen, G. *Chem. Commun.* **2012**, *48*, 12207−12209.
(10) Tang, D.; Yuan, R.; Chai, Y. *Anal. Chem.* **2008**, *80*, 1582−1588.
(11) Tang, D.; Yuan, R.; Chai, Y. *Clin. Chem.* **2007**, *53*, 1323−1329.
(12) Huang, J.; Wu, Y.; Chen, Y.; Zhu, Z.; Yang, X.; Yang, C.; Wang, K.; Tan, W. *Angew. Chem., Int. Ed.* **2011**, *50*, 401−404.
(13) Ji, H.; Yan, F.; Lei, J.; Ju, H. *Anal. Chem.* **2012**, *84*, 7166−7171.
(14) Schweller, R.; Zimak, J.; Duose, D.; Qutub, A.; Hittelman, W.; Diehl, M. *Angew. Chem., Int. Ed.* **2012**, *51*, 9292−9296.
(15) Merchlinsky, M.; Moss, B. *J. Virol.* **1989**, *63*, 1595−1603.
(16) Chen, X.; Lin, Y.; Li, J.; Lin, L.; Chen, G.; Yang, H. *Chem. Commun.* **2011**, *47*, 12116−12118.
(17) Dirks, R.; Pierce, N. *Proc. Natl. Acad. Sci. U.S.A.* **2004**, *101*, 15275−15278.
(18) Chen, X.; Hong, C.; Lin, Y.; Chen, J.; Chen, G.; Yang, H. *Anal. Chem.* **2012**, *84*, 8277−8283.
(19) Tang, J.; Hou, L.; Tang, D.; Zhang, B.; Zhou, J.; Chen, G. *Chem. Commun.* **2012**, *48*, 8180−8182.
(20) Xiang, Y.; Lu, Y. *Anal. Chem.* **2012**, *84*, 9981−9987.
(21) Lu, C.; Wang, F.; Willner, I. *J. Am. Chem. Soc.* **2012**, *134*, 10651−10658.
(22) Yuan, Y.; Yuan, R.; Chai, Y.; Zhuo, Y.; Ye, X.; Gan, X.; Bai, L. *Chem. Commun.* **2012**, *48*, 4621−4623.
(23) Tang, J.; Tang, D.; Niessner, R.; Chen, G.; Knopp, D. *Anal. Chem.* **2011**, *83*, 5407−5414.
(24) Tang, D.; Ren, J. *Anal. Chem.* **2008**, *80*, 8064−8070.
(25) Rohs, R.; Sklenar, H. *J. Biomol. Struct. Dyn.* **2004**, *21*, 699−711.
(26) Wang, J.; Hogan, M.; Austin, R. *Proc. Natl. Acad. Sci. U.S.A.* **1982**, *79*, 5896−5900.
(27) Hogan, M.; Wang, J.; Austin, R.; Monitto, C.; Hershkowitz, S. *Proc. Natl. Acad. Sci. U.S.A.* **1982**, *79*, 3518−3522.

(28) Yuan, R.; Tang, D.; Chai, Y.; Zhong, X.; Liu, Y.; Dai, J. *Langmuir* **2004**, *20*, 7240−7245.
(29) Yan, J.; Su, S.; He, S.; He, Y.; Zhao, B.; Wang, D.; Zhang, Q.; Song, S.; Fuan, C. *Anal. Chem.* **2012**, *84*, 9139−9145.
(30) Tang, D.; Yuan, R.; Chai, Y. *Electroanalysis* **2006**, *18*, 259−266.
(31) Olmsted, I.; Kussrow, A.; Bornhop, D. *Anal. Chem.* **2012**, *84*, 10817−10822.
(32) Chakrabary, R.; Stang, P. *J. Am. Chem. Soc.* **2012**, *134*, 14738−14741.
(33) Tang, J.; Hou, L.; Tang, D.; Zhang, B.; Zhou, J.; Chen, G. *Chem. Commun.* **2012**, *48*, 8180−8182.
(34) Zeng, L.; Li, Q.; Tang, D.; Chen, G.; Wei, M. *Electrochim. Acta* **2012**, *68*, 158−165.
(35) Ikura, K.; Fujimoto, J.; Kubonishi, K.; Natsuka, S.; Hashimoto, H.; Ito, T.; Fujita, K. *Cytotechnology* **2002**, *40*, 23−29.
(36) Chen, J.; Tang, J.; Yan, F.; Ju, H. *Biomaterial* **2006**, *27*, 2313−2321.
(37) Eteshola, E.; Keener, M.; Elias, M.; Shapiro, J.; Brillson, L.; Bhushan, B.; Lee, S. *J. R. Soc. Interface* **2008**, *5*, 123−127.
(38) Hendrickson, W.; Pahler, A.; Smith, J.; Satow, Y.; Merritt, E.; Phizackerley, R. *Proc. Natl. Acad. Sci. U.S.A.* **1989**, *86*, 2190−2194.
(39) Wang, J. *Proc. Natl. Acad. Sci. U.S.A.* **1979**, *76*, 200−203.
(40) Zhang, B.; Tang, D.; Goryacheva, I.; Niessner, R.; Knopp, D. *Chem.—Eur. J.* **2013**, DOI: 10.1002/chem..201203131.